

Distribution of the Sum of Fisher-Snedecor \mathcal{F}

Random Variables and Its Applications

Hongyang Du, Jiayi Zhang, *Member, IEEE*, Julian Cheng, *Senior Member, IEEE*,
and Bo Ai, *Senior Member, IEEE*

Abstract

The statistical characterization of the sum of random variables (RVs) are useful for investigating the performance of wireless communication systems. We derive exact closed-form expressions for the probability density function (PDF) and cumulative distribution function (CDF) of a sum of independent but not identically distributed (i.n.i.d.) Fisher-Snedecor \mathcal{F} RVs. Both PDF and CDF are given in terms of the multivariate Fox's H -function. Besides, a simple and accurate approximation to the sum of i.n.i.d. Fisher-Snedecor \mathcal{F} variates is presented using the moment matching method. The obtained PDF and CDF are used to evaluate the performance of wireless communication applications including the outage probability, the effective capacity and the channel capacities under four different adaptive transmission strategies. Moreover, the corresponding approximate expressions are obtained to provide useful insights for the design and deployment of wireless communication systems. In addition, we derive simple asymptotic expressions for the proposed mathematical analysis in the high signal-to-noise ratio regime. Finally, the numerical results demonstrate the accuracy of the derived expressions.

Index Terms

Channel capacity, effective capacity, Fisher-Snedecor \mathcal{F} -distribution, sum of random variables,

I. INTRODUCTION

Recently, the Fisher-Snedecor \mathcal{F} distribution was proposed [1] as a tractable fading model to describe the combined effects of shadowing and multipath fading. This distribution can be reduced to some common

H. Du and J. Zhang are with the School of Electronic and Information Engineering, Beijing Jiaotong University, Beijing 100044, P. R. China. (e-mail: {17211140; jiayizhang }@bjtu.edu.cn)

J. Cheng is with the School of Engineering, The University of British Columbia, Kelowna, BC V1V 1V7, Canada.

B. Ai is with the State Key Laboratory of Rail Traffic Control and Safety, Beijing Jiaotong University, Beijing 100044, China (e-mail: boai@bjtu.edu.cn).

fading models, such as Nakagami- m and Rayleigh fading channels. Furthermore, it is found in [1] that the \mathcal{F} distribution can provide a better fit to the experimental data obtained for device-to-device (D2D) and wearable communication links, especially at 5.8 GHz, as compared with the well established generalized- K (GK) distribution. In addition, its probability density function (PDF) consists of only elementary functions and it leads to more tractable analysis than the GK model [1]. Due to its promising properties, the performance of digital communication systems over \mathcal{F} distributed fading channels has been analyzed in [2]–[5] and the references therein.

The sum of random variables (RVs) has a wide range of important applications in the performance analysis of wireless communication systems. For example, to enhance the quality of the received signal, maximal-ratio combining (MRC) can be deployed at the receiver to maximize the combiner output signal-to-noise ratio (SNR) [6]. The system with MRC receiver operating over different fading channels has been extensively studied [7]–[12].

The PDF and CDF of the sum of Fisher-Snedecor \mathcal{F} RVs has been derived in terms of Lauricella multivariate hypergeometric function [13]. However, these results are difficult to be used in the performance analysis of MRC systems over Fisher-Snedecor \mathcal{F} fading channels due to the complexity of the Lauricella multivariate hypergeometric function. Moreover, authors in [13] obtain outage probability (OP) and outage capacity expressions involving L -fold Mellin-Barnes type contour integral, where L is the number of diversity branches. These results cannot be calculated efficiently, thus the insights into the system performance are limited. Moreover, the statistical characterization is challenging, if not impossible, to derive the important performance metrics, such as channel capacity and effective capacity.

In order to fill this gap, we re-investigate the statistical characterization of the statistical characterization of the sum of independent but not identically distributed (i.n.i.d.) Fisher-Snedecor \mathcal{F} RVs and leverage the PDF and CDF expressions to analyze the performance of the MRC receiver in terms of outage probability, channel capacity and effective capacity [14]–[17].

The main contributions of this paper are summarized as follows:

- We derive exact closed-form expressions for the PDF and cumulative distribution function (CDF) of the sum of i.n.i.d. Fisher-Snedecor \mathcal{F} RVs in terms of the multivariate Fox's H -function, which can be efficiently programmed in standard software packages (e.g., Maple and Mathematica) [21–24].
- We introduce a paradigm based on the moment matching method to obtain a simple approximation to the sum of Fisher-Snedecor \mathcal{F} RVs using another single \mathcal{F} RV. To improve the accuracy of the

approximation, we propose an adjustment factor to modify the error in the lower and upper tail regions. The approximated expression is easier to evaluate in the performance analysis. We employ the Kolmogorov-Smirnov (KS) goodness-of-fit statistical test to show that the single \mathcal{F} distribution is a highly accurate approximation to the sum of \mathcal{F} RVs.

- We derive novel analytical expressions for important performance metrics, namely the OP, the effective capacity and the channel capacities under four different adaptive transmission schemes, including optimal rate adaptation with constant transmit power (ORA), simultaneous optimal power and rate adaptation (OPRA), channel inversion with fixed rate (CIFR) and truncated channel inversion with fixed rate (TIFR). Moreover, the final value theorem is used to avoid the conflict between the definition of the multivariate Fox's H -function and the analytical expressions.
- We derive highly accurate and simplified closed-form approximations for the studied performance metrics by using a single \mathcal{F} distribution. Furthermore, we pursue an asymptotic performance analysis in the high-SNR regime. The derived results can provide useful insights into the effects of different system and fading parameters on the performance.

The remainder of the paper is organized as follows. In Section II, we introduce the statistical characterizations of the \mathcal{F} distribution and the definition of multivariable Fox's H function. Exact closed-form PDF and CDF expressions of the sum of Fisher-Snedecor \mathcal{F} RVs are derived in Section III. Section IV provides a single \mathcal{F} distribution to approximate the distribution of sum of \mathcal{F} RVs using the moment matching method for the first, second and third moments, and the KS goodness-of-fit statistical test is evaluated. In Section V, we investigate the performance in several wireless communications scenarios, and present simple asymptotic expressions. Section VI provides the numerical results and the accuracy of the obtained expressions is validated via Monte Carlo simulations. Finally, Section VII concludes this paper.

II. PRELIMINARIES

A. Statistics of Fisher-Snedecor \mathcal{F} Random Variables

The PDF and CDF of the instantaneous SNR, γ , at the destination over Fisher-Snedecor \mathcal{F} fading channels are respectively given by [18, eq. (6)], [18, eq. (12)].

$$f_{\gamma}(\gamma) = \frac{m^m (m_s - 1)^{m_s} \bar{\gamma}^{m_s} \gamma^{m-1}}{B(m, m_s) (m\gamma + (m_s - 1)\bar{\gamma})^{m+m_s}}, \quad (1)$$

and

$$F_\gamma(\gamma) = \frac{m^{m-1}\gamma^m}{B(m, m_s)(m_s - 1)^{m\bar{\gamma}}m} {}_2F_1\left(m, m + m_s, m + 1; -\frac{m\gamma}{(m_s - 1)\bar{\gamma}}\right) \quad (2)$$

where $B(\cdot, \cdot)$ denotes the beta function [19, eq. (8.38)]; ${}_2F_1(\cdot)$ denotes the Gauss hypergeometric function [19, eq. (9.10)] and $m_s > 1$; the parameters m , m_s , and $\bar{\gamma}$ denote the number of multipath clusters, shadowing shape, and average SNR, respectively

The MGF of γ is given by [18, eq. (10)]

$$\mathcal{M}_\gamma(s) = {}_1F_1\left(m; 1 - m_s; \frac{s\bar{\gamma}(m_s - 1)}{m}\right) + \frac{\Gamma(-m_s)\left(\frac{s\bar{\gamma}(m_s - 1)}{m}\right)^{m_s}}{B(m, m_s)} {}_1F_1\left(m + m_s; 1 + m_s; \frac{s\bar{\gamma}(m_s - 1)}{m}\right) \quad (3)$$

where ${}_1F_1(\cdot, \cdot, \cdot)$ denotes the Kummer confluent hypergeometric function [19, eq. (9.210.1)]. With the definition of Tricomis confluent hypergeometric function [19, eq. (9.210.2)] and after some algebraic manipulations, we obtain

$$\mathcal{M}_\gamma(s) = \frac{\Gamma(m + m_s)}{\Gamma(m_s)} \Psi\left(m, 1 - m_s; \frac{s\bar{\gamma}(m_s - 1)}{m}\right) \quad (4)$$

where $\Psi(\cdot, \cdot; \cdot)$ is the Tricomis confluent hypergeometric function, which can be expressed as the Meijer G -function [19, eq. (8.4.3.1)], and (4) can be written as eq. (2) in [13].

The n th moment of the Fisher-Snedecor \mathcal{F} distribution can be derived in closed-form as [18, eq. (9)]. With the aid of [19, eq. (8.384.1)], one obtains

$$\mathbb{E}[\gamma^n] = \left(\frac{(m_s - 1)\bar{\gamma}}{m}\right)^n \frac{B(m + n, m_s - n)}{B(m, m_s)} \quad (5)$$

where $\mathbb{E}[\cdot]$ denotes the mathematical expectation.

B. Multivariable Fox's H -function

Multivariable Fox's H -function has several notations. Among them, we choose a widely adopted notation given as [20, eq. (A.1)]

$$\begin{aligned}
 H[z_1, \dots, z_r] &\triangleq H_{p,q;p_1,q_1;\dots;p_r,q_r}^{0,n;m_1,n_1;\dots;m_r,n_r} \left[\begin{array}{c} z_1 \\ \vdots \\ z_r \end{array} \middle| \begin{array}{c} (a_j; \alpha_j^{(1)}, \dots, \alpha_j^{(r)})_{1,p} : (c_j^{(1)}, \gamma_j^{(1)})_{1,p_1}; \dots; (c_j^{(r)}, \gamma_j^{(r)})_{1,p_r} \\ (b_j; \beta_j^{(1)}, \dots, \beta_j^{(r)})_{1,q} : (d_j^{(1)}, \delta_j^{(1)})_{1,q_1}; \dots; (d_j^{(r)}, \delta_j^{(r)})_{1,q_r} \end{array} \right] \\
 &= \frac{1}{(2\pi j)^r} \int_{L_1} \cdots \int_{L_r} \Psi(\zeta_1, \dots, \zeta_r) \left\{ \prod_{i=1}^r \phi_i(\zeta_i) z_i^{\zeta_i} \right\} d\zeta_1 \cdots d\zeta_r \quad (6)
 \end{aligned}$$

where $j \triangleq \sqrt{-1}$,

$$\Psi(\zeta_1, \dots, \zeta_r) = \frac{\prod_{j=1}^n \Gamma\left(1 - a_j + \sum_{i=1}^r \alpha_j^{(i)} \zeta_i\right)}{\left[\prod_{j=n+1}^p \Gamma\left(a_j - \sum_{i=1}^r \alpha_j^{(i)} \zeta_i\right) \right] \left[\prod_{j=1}^q \Gamma\left(1 - b_j + \sum_{i=1}^r \beta_j^{(i)} \zeta_i\right) \right]}, \quad (7a)$$

$$\phi_i(\zeta_i) = \frac{\left[\prod_{\lambda=1}^{m_i} \Gamma\left(d_\lambda^{(i)} - \delta_\lambda^{(i)} \zeta_i\right) \right] \left[\prod_{j=1}^{n_i} \Gamma\left(1 - c_j^{(i)} + \gamma_j^{(i)} \zeta_i\right) \right]}{\left[\prod_{j=n_i+1}^{p_i} \Gamma\left(c_j^{(i)} - \gamma_j^{(i)} \zeta_i\right) \right] \left[\prod_{\lambda=m_i+1}^{q_i} \Gamma\left(1 - d_\lambda^{(i)} + \delta_\lambda^{(i)} \zeta_i\right) \right]}. \quad (7b)$$

Although the numerical evaluation for multivariate Fox's H -function is not available in popular mathematical packages such as MATLAB and Mathematica, its efficient implementations have been reported. For example, two Mathematica implementations of the single Fox's H -function are provided in [14] and [15], a Python implementation for the multivariable Fox's H -function is presented in [16], and an efficient GPU-oriented MATLAB routine for the multivariate Fox's H -function is introduced in [17]. In the following, we will utilize these novel implementations to evaluate our results.

III. SUM OF FISHER-SNEDECOR \mathcal{F} RANDOM VARIABLES

In this section, we investigate the statistical characterization of the sum of Fisher-Snedecor \mathcal{F} RVs and derive exact closed-form expressions for PDF and CDF. Let $z \triangleq \gamma_1 + \gamma_2 + \cdots + \gamma_L$, where $\gamma_\ell \sim \mathcal{F}(\bar{\gamma}_\ell, m_\ell, m_{s_\ell})$ ($\ell = 1, \dots, L$) are i.n.i.d. Fisher-Snedecor \mathcal{F} RVs.

Theorem 1. *The PDF of the sum of Fisher-Snedecor \mathcal{F} RVs z is given by*

$$f_Z(z) = \frac{1}{z \prod_{\ell=1}^L \Gamma(m_\ell) \Gamma(m_{s_\ell})} H_{\text{PDF}} \quad (8)$$

where

$$H_{\text{PDF}} \triangleq H_{0,1:2,1;2,1;\dots;2,1}^{0,0:1,2;1,2;\dots;1,2} \left(\begin{array}{c} \frac{m_1 z}{(m_{s_1}-1)\bar{\gamma}_1} \\ \vdots \\ \frac{m_L z}{(m_{s_L}-1)\bar{\gamma}_L} \end{array} \middle| \begin{array}{l} - : (1, 1), (1-m_{s_1}, 1); \dots; (1, 1), (1-m_{s_L}, 1) \\ (1; 1, \dots, 1) : (m_1, 1); \dots; (m_L, 1) \end{array} \right). \quad (9)$$

Proof: Please refer to Appendix A. ■

Theorem 2. *The CDF of the sum of Fisher-Snedecor \mathcal{F} RVs z is given by*

$$F_Z(z) = \frac{1}{\prod_{\ell=1}^L \Gamma(m_\ell) \Gamma(m_{s_\ell})} H_{\text{CDF}} \quad (10)$$

where

$$H_{\text{CDF}} \triangleq H_{0,1:2,1;2,1;\dots;2,1}^{0,0:1,2;1,2;\dots;1,2} \left(\begin{array}{c} \frac{m_1 z}{(m_{s_1}-1)\bar{\gamma}_1} \\ \vdots \\ \frac{m_L z}{(m_{s_L}-1)\bar{\gamma}_L} \end{array} \middle| \begin{array}{l} - : (1, 1), (1-m_{s_1}, 1); \dots; (1, 1), (1-m_{s_L}, 1) \\ (0; 1, \dots, 1) : (m_1, 1); \dots; (m_L, 1) \end{array} \right) \quad (11)$$

Proof: Following similar procedures as in Appendix A, we can derive the CDF of z by taking the inverse Laplace transform of $M_z(s)/s$. ■

IV. ACCURATE CLOSED-FORM APPROXIMATIONS

In this section, we present accurate closed-form approximations to the distribution of a sum of Fisher-Snedecor \mathcal{F} RVs using a single Fisher-Snedecor \mathcal{F} RV, which can be used to provide more insights into the impact of the parameters on the overall system performance. The parameters $\bar{\gamma}$, $m_{\mathcal{F}}$ and $m_{s_{\mathcal{F}}}$ are obtained using the moment matching method for the first, second and third moments.

A. Single \mathcal{F} Approximation to the sum of Squared \mathcal{F} -distributed RVs

Theorem 3. For the sum of i.n.i.d. \mathcal{F} RVs, the parameters of single \mathcal{F} distribution are given by

$$\begin{cases} \bar{\gamma}_{\mathcal{F}} = \sum_{i=1}^L \bar{\gamma}_i, \\ m_{\mathcal{F}} = -\frac{2(H_{\mathcal{F}} - Y_{\mathcal{F}})}{H_{\mathcal{F}} - 2Y_{\mathcal{F}} + H_{\mathcal{F}}Y_{\mathcal{F}}}, \\ m_{s_{\mathcal{F}}} = \frac{4H_{\mathcal{F}} - 3Y_{\mathcal{F}} - 1}{2H_{\mathcal{F}} - Y_{\mathcal{F}} - 1} \end{cases} \quad (12)$$

where $H_{\mathcal{F}}$ and $Y_{\mathcal{F}}$ can be calculated as

$$\begin{cases} H_{\mathcal{F}} \triangleq \frac{\sum_{\ell=1}^L (H_{\ell} - \varepsilon_{\ell} - 1) \bar{\gamma}_{\ell}^2}{\left(\sum_{\ell=1}^L \bar{\gamma}_{\ell}\right)^2} + 1, \\ Y_{\mathcal{F}} \triangleq \frac{\sum_{\ell=1}^L (H_{\ell} Y_{\ell} - \varepsilon_{\ell} Y_{\ell} - 1) \bar{\gamma}_{\ell}^3 + \left(\sum_{\ell=1}^L \bar{\gamma}_{\ell}\right)^3 + 3 \left(\sum_{\ell=1}^L \bar{\gamma}_{\ell}\right) \left(\sum_{\ell=1}^L (H_{\ell} - \varepsilon_{\ell} - 1) \bar{\gamma}_{\ell}^2\right) - 3 \sum_{\ell=1}^L (H_{\ell} - \varepsilon_{\ell} - 1) \bar{\gamma}_{\ell}^3}{\left(\sum_{\ell=1}^L \bar{\gamma}_{\ell}\right) \left(\sum_{\ell=1}^L (H_{\ell} - \varepsilon_{\ell} - 1) \bar{\gamma}_{\ell}^2 + \left(\sum_{\ell=1}^L \bar{\gamma}_{\ell}\right)^2\right)} \end{cases} \quad (13)$$

where $H_{\ell} = \frac{(1+m_{\ell})(m_{s_{\ell}}-1)}{m_{\ell}(m_{s_{\ell}}-2)}$ ($\ell = 1, \dots, L$), $Y_{\ell} = \frac{(m_{s_{\ell}}-1)(2+m_{\ell})}{m_{\ell}(m_{s_{\ell}}-3)}$ and ε_{ℓ} is the factor that can be adjusted to minimize the difference between the approximate and the exact statistics. For example, we can choose ε_{ℓ} to minimize the Kolmogorov distance.

For the i.i.d case, let $H_{\ell} = H$ ($\ell = 1, \dots, L$), $Y_{\ell} = Y$, $m = m_{\ell}$, $m_s = m_{s_{\ell}}$, $\varepsilon = \varepsilon_{\ell}$, $\bar{\gamma} = \bar{\gamma}_{\ell}$, so the parameters of single \mathcal{F} distribution are given by

$$\begin{cases} \bar{\gamma}_{\mathcal{F}} = L\bar{\gamma}, \\ m_{\mathcal{F}} = -\frac{2(H_{\mathcal{F}} - Y_{\mathcal{F}})}{H_{\mathcal{F}} - 2Y_{\mathcal{F}} + H_{\mathcal{F}}Y_{\mathcal{F}}}, \\ m_{s_{\mathcal{F}}} = \frac{4H_{\mathcal{F}} - 3Y_{\mathcal{F}} - 1}{2H_{\mathcal{F}} - Y_{\mathcal{F}} - 1} \end{cases} \quad (14)$$

where

$$\begin{cases} H_{\mathcal{F}} \triangleq \frac{(H - \varepsilon - 1)}{L} + 1, \\ Y_{\mathcal{F}} \triangleq \frac{(H - \varepsilon)Y + L^2 + 3L(H - \varepsilon) - 3L - 3(H - \varepsilon) + 2}{L(H - \varepsilon) - L + L^2}. \end{cases} \quad (15)$$

Proof: Please refer to Appendix B. ■

B. KS Goodness-of-fit Test

KS goodness-of-fit statistical test can be used to test the accuracy of the proposed approximations [21]. The KS test is defined as the largest absolute difference between two CDFs, which can be expressed as

$$T \triangleq \max |F_Z(z) - F_{\hat{Z}}(z)| \quad (16)$$

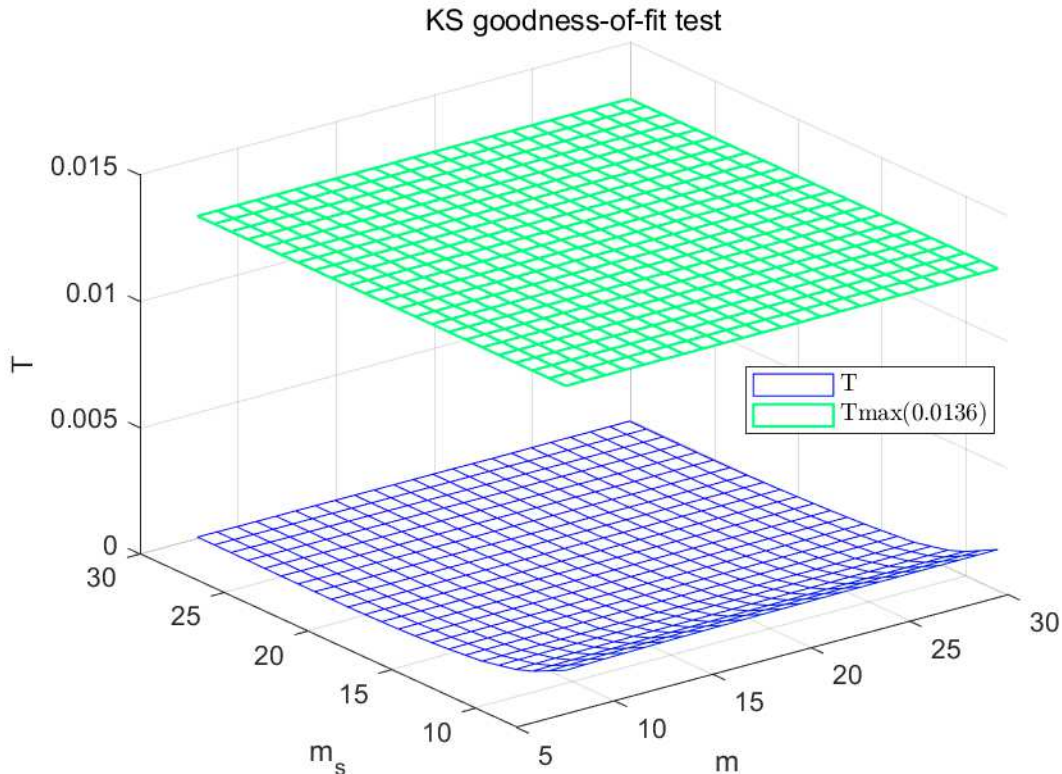


Fig. 1. KS goodness-of-fit test statistic for the exact and the approximate distributions with 5% significance level for $L = 2$.

where $F_Z(z)$ is the analytical CDF of RV Z and $F_{\hat{Z}}(z)$ is the empirical CDF of RV \hat{Z} .

Let us define H_0 as the null hypothesis under which the observed data of \hat{Z} belong to the CDF of the approximate distribution $F_Z(z)$. Hypothesis H_0 is accepted if $T < T_{\max}$. The critical value $T_{\max} = \sqrt{-(1/2v) \ln(\alpha/2)}$ corresponds to a significance level of α [21].

Without loss of generality, we consider a sum of two i.i.d. Fisher-Snedecor \mathcal{F} RVs with channel parameters $m = m_\ell$ and $m_s = m_{s_\ell}$ ($\ell = 1, 2$). The average SNR is set by $\bar{\gamma} = \bar{\gamma}_\ell = 1$ dB. The exact results of CDF have been obtained by averaging at least $v = 10^4$, and one obtains $T_{\max} = 0.0136$ for $\alpha = 5\%$. Fig. 1 depicts the KS test statistic for different combinations of m and m_s , and the corresponding optimal adjustment factor ε is shown in the Fig. 2. It is obvious that H_0 is accepted with 95% significance for different settings of parameters. In conclusion, the single \mathcal{F} distribution is a highly accurate approximation to the sum of \mathcal{F} RVs.

V. APPLICATIONS TO WIRELESS COMMUNICATIONS

In this section, we present six applications in wireless communication systems, including OP, effective capacity, and channel capacities under four different adaptive transmission strategies. We assume com-

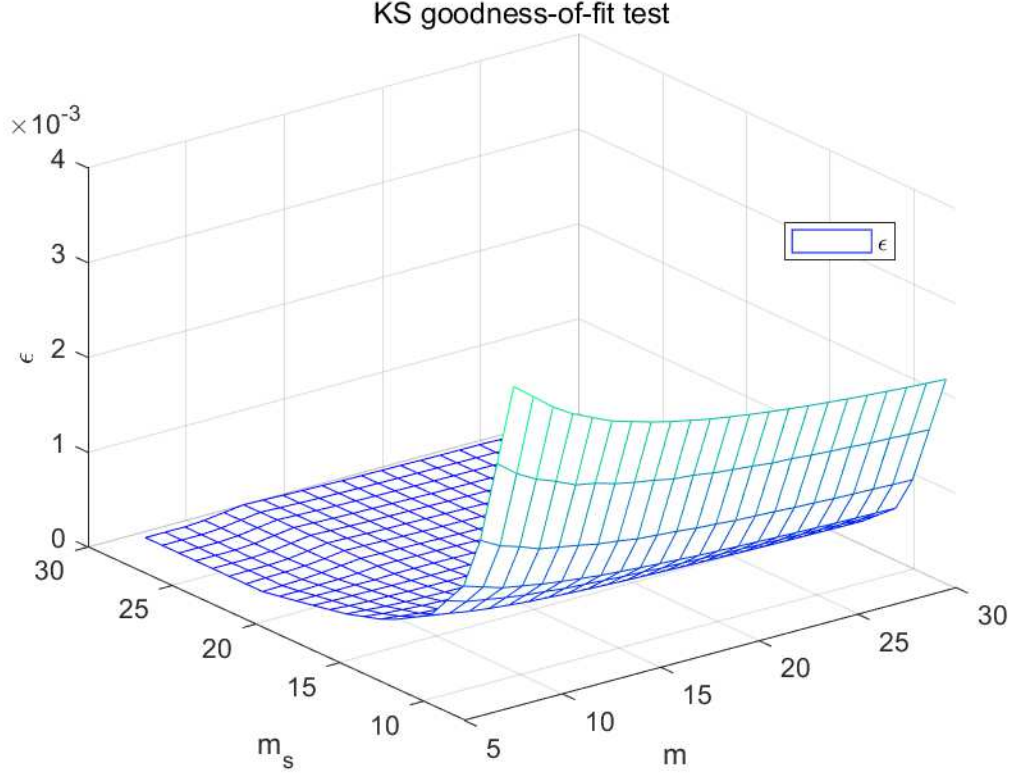


Fig. 2. Adjustment factor that minimizes the absolute value of the difference between the exact and the approximate distributions for $L = 2$.

munication over a fading channel that follows Fisher-Snedecor \mathcal{F} distribution and a diversity receiver employs MRC.

A. Outage Probability

The OP is defined as the probability that the instantaneous SNR is less than a predetermined threshold γ_{th} . The combiner output SNR Z is simply the sum of the individual branches SNRs and the OP can be directly calculated as

$$P_{\text{out}} = P(Z < \gamma_{\text{th}}) = F_Z(\gamma_{\text{th}}) \quad (17)$$

where γ_{th} is the minimum usable SNR threshold. Therefore, the OP of the MRC receiver can be directly evaluated by using (10).

Proposition 1. *A highly accurate and simple approximation of OP can be derived using single \mathcal{F} fading channel as*

$$P_{o,\mathcal{F}} \simeq \frac{m_{\mathcal{F}}^{m_{\mathcal{F}}-1} \gamma_{\text{th}}^{m_{\mathcal{F}}}}{B(m_{\mathcal{F}}, m_{s_{\mathcal{F}}}) (m_{s_{\mathcal{F}}} - 1)^{m_{\mathcal{F}}} \bar{\gamma}_{\mathcal{F}}^{m_{\mathcal{F}}}} {}_2F_1 \left(m_{\mathcal{F}}, m_{\mathcal{F}} + m_{s_{\mathcal{F}}}, m_{\mathcal{F}} + 1; -\frac{m_{\mathcal{F}} \gamma_{\text{th}}}{(m_{s_{\mathcal{F}}} - 1) \bar{\gamma}_{\mathcal{F}}} \right). \quad (18)$$

The asymptotic expansions of the OP for high SNRs can be obtained by computing the residue [16]. Let us consider the residue at the points $\zeta = (\zeta_1, \dots, \zeta_L)$, where $\zeta_\ell = \min_{j=1, \dots, m_\ell} \left(d_j^{(\ell)} / \delta_j^{(\ell)} \right)$ ($\ell = 1, \dots, L$). We obtain the approximate OP expression as

$$P_{o, \text{appr}} \simeq \frac{1}{\Gamma \left(1 + \sum_{\ell=1}^L m_\ell \right)} \prod_{\ell=1}^L \frac{\Gamma(m_{s_\ell} + m_\ell)}{\Gamma(m_{s_\ell})} \left(\frac{\gamma_{\text{th}} m_\ell}{\bar{\gamma}_\ell (m_{s_\ell} - 1)} \right)^{m_\ell}. \quad (19)$$

B. Effective Capacity

The effective capacity, which accounts for the achievable capacity subject to the incurred latency relating to the corresponding buffer occupancy, is a useful and insightful information theoretic measure particularly in emerging technologies. The effective capacity normalised by the bandwidth can be defined as [22, eq. (11)]

$$C_{\text{eff}} = -\frac{1}{A} \log_2 \left(\int_0^\infty \frac{1}{(1+z)^A} f_z(z) dz \right) \quad \text{bit/s/Hz} \quad (20)$$

where $z = \sum_{\ell=1}^L \gamma_\ell$, $\gamma_\ell \sim \mathcal{F}(\bar{\gamma}_\ell, m_\ell, m_{s_\ell})$ ($\ell = 1, \dots, L$), and

$$A = \frac{BT\theta}{\ln 2} \quad (21)$$

is a delay constraint with the asymptotic decay rate of the buffer occupancy θ , system bandwidth B and the block length T .

Proposition 2. For the i.n.i.d. case, the effective capacity can be deduced as

$$C_{\text{eff}} = -\frac{1}{A} \log_2 \left(\frac{A}{\Gamma(1+A)} \prod_{\ell=1}^L \frac{1}{\Gamma(m_\ell) \Gamma(m_{s_\ell})} H_{\text{eff}} \right), \quad (22)$$

where

$$H_{\text{eff}} \triangleq H_{1,0:2,1;\dots;2,1}^{0,1:1,2;\dots;1,2} \left(\begin{array}{c} \frac{m_1}{(m_{s_1}-1)\bar{\gamma}_1} \\ \vdots \\ \frac{m_L}{(m_{s_L}-1)\bar{\gamma}_L} \end{array} \middle| \begin{array}{c} (1-A; -1, \dots, -1) : (1, 1), (1-m_{s_1}, 1); \dots; (1, 1), (1-m_{s_L}, 1) \\ - : (m_1, 1); \dots; (m_L, 1) \end{array} \right), \quad (23)$$

Proof: Using the classical Newton-Leibniz formula, we can rewrite (20) as

$$\begin{aligned} C_{\text{eff}} &= -\frac{1}{A} \log_2 \left(\int_0^\infty \frac{1}{(1+z)^A} f_z(z) dz \right) = -\frac{1}{A} \log_2 \left(\int_0^\infty \frac{1}{(1+z)^A} dF_Z(z) \right) \\ &= -\frac{1}{A} \log_2 \left(\underbrace{A \int_0^\infty \frac{F_z(z)}{(1+z)^{A+1}} dz}_{I_1} \right). \end{aligned} \quad (24)$$

With the help of (10), I_1 can be expressed as

$$\begin{aligned} I_1 &= \prod_{\ell=1}^L \frac{1}{\Gamma(m_\ell) \Gamma(m_{s_\ell})} \left(\frac{1}{2\pi j} \right)^L \\ &\times \int_0^\infty \frac{1}{(1+z)^{A+1}} \int_{\mathcal{L}_1} \int_{\mathcal{L}_2} \cdots \int_{\mathcal{L}_L} \frac{1}{\Gamma\left(1 + \sum_{\ell=1}^L \zeta_\ell\right)} \left\{ \prod_{\ell=1}^L \Upsilon(\zeta_\ell) \left(\frac{zm_\ell}{\bar{\gamma}_\ell(m_{s_\ell} - 1)} \right)^{-\zeta_\ell} \right\} d\zeta_1 d\zeta_2 \cdots d\zeta_L dz \end{aligned} \quad (25)$$

where $\Upsilon(\zeta_\ell) = \Gamma(m_\ell - \zeta_\ell) \Gamma(\zeta_\ell) \Gamma(m_{s_\ell} + \zeta_\ell)$. According to Fubini's theorem, we can exchange the order of integrations in I_1 , and derive

$$\begin{aligned} I_1 &= \prod_{\ell=1}^L \frac{1}{\Gamma(m_\ell) \Gamma(m_{s_\ell})} \left(\frac{1}{2\pi j} \right)^L \\ &\times \int_{\mathcal{L}_1} \int_{\mathcal{L}_2} \cdots \int_{\mathcal{L}_L} \frac{1}{\Gamma\left(1 + \sum_{\ell=1}^L \zeta_\ell\right)} \left\{ \prod_{\ell=1}^L \Upsilon(\zeta_\ell) \left(\frac{m_\ell}{\bar{\gamma}_\ell(m_{s_\ell} - 1)} \right)^{-\zeta_\ell} \right\} \underbrace{\int_0^\infty \frac{z^{\sum_{\ell=1}^L \zeta_\ell}}{(1+z)^{A+1}} dz}_{I_2} d\zeta_1 d\zeta_2 \cdots d\zeta_L. \end{aligned} \quad (26)$$

Using [19, eq. (3.194.3)], we can solve I_2 as

$$I_2 = \frac{\Gamma\left(\sum_{\ell=1}^L \zeta_\ell + 1\right) \Gamma\left(A - \sum_{\ell=1}^L \zeta_\ell\right)}{\Gamma(1+A)}. \quad (27)$$

Combining (27), (26), (24) and (6), we obtain (22) to complete the proof. \blacksquare

Remark 1. A highly accurate approximation of effective capacity can be derived using a single \mathcal{F} fading channel by setting $L = 1$ in (22). After some algebraic manipulations, we obtain the same result as [18, eq. (33)] which provides useful insights because it can be used as a benchmark for the derivation of simpler approximations or bounds. The approximation of effective capacity in the high SNR region under

\mathcal{F} fading channels was also derived as [18, eq. (41)], which can be used as the approximation of (22).

C. Channel Capacity

Channel capacity is a key performance metric in communication systems. In the following, we analyze the channel capacity performance under four different adaptive transmission schemes, namely CIFR, TIFR, ORA and OPRA.

1) *Channel Inversion with Fixed Rate*: CIFR ensures a fixed data rate at the receiver by inverting the channel and adapting the transmit power. The channel capacity under CIFR is defined in [23] as

$$C_{\text{CIFR}} = B \log_2 \left(1 + \frac{1}{\int_0^\infty \frac{f_Z(z)}{z} dz} \right). \quad (28)$$

Proposition 3. *The channel capacity under CIFR can be expressed as*

$$C_{\text{CIFR}} = B \log_2 \left(1 + \frac{1}{\prod_{\ell=1}^L \frac{s}{\Gamma(m_{s_\ell}) \Gamma(m_\ell)} H_{\text{CIFR}}} \right) \quad (29)$$

where

$$H_{\text{CIFR}} \triangleq H_{1,0;2,1;\dots;2,1}^{0,1;1,2;\dots;1,2} \left(\begin{array}{c} \frac{m_1}{s(m_{s_1}-1)\bar{\gamma}_1} \\ \vdots \\ \frac{m_L}{s(m_{s_L}-1)\bar{\gamma}_L} \end{array} \middle| \begin{array}{l} (2; 1, \dots, 1) : (1, 1), (1 - m_{s_1}, 1); \dots; (1, 1), (1 - m_{s_L}, 1) \\ (1; 1, \dots, 1) : (m_1, 1); \dots; (m_L, 1) \end{array} \right) \quad (30)$$

and s is a number close to zero (e.g., $s = 10^{-6}$).

Proof: With the aid of (8), the integral in (28) can be written as

$$I_3 = \prod_{\ell=1}^L \frac{1}{\Gamma(m_{s_\ell}) \Gamma(m_\ell)} \left(\frac{1}{2\pi i} \right)^L \\ \times \int_0^\infty \int_{\mathcal{L}_1} \int_{\mathcal{L}_2} \dots \int_{\mathcal{L}_L} \prod_{\ell=1}^L \Upsilon(\zeta_\ell) \left(\frac{m_\ell}{\bar{\gamma}_\ell (m_{s_\ell} - 1)} \right)^{\zeta_\ell} \frac{1}{\Gamma\left(\sum_{\ell=1}^L \zeta_\ell\right)} z^{-2 + \sum_{\ell=1}^L \zeta_\ell} d\zeta_1 d\zeta_2 \dots d\zeta_L dz. \quad (31)$$

Let $\mathcal{L}\{p(t)\} = P(x)$. According to the property of Laplace transform, we have

$$\mathcal{L} \left\{ \int_0^t p(z) dz \right\} = \frac{P(x)}{x}. \quad (32)$$

With the help of the final value theorem, it follows that

$$\lim_{t \rightarrow \infty} \left(\int_0^t p(z) dz \right) = s \frac{P(s)}{s} = P(s). \quad (33)$$

We can use (33) to obtain

$$\int_0^\infty z^{-2 + \sum_{\ell=1}^L \zeta_\ell} dz = \mathcal{L} \left\{ z^{-2 + \sum_{\ell=1}^L \zeta_\ell} \right\} = \left(\frac{1}{s} \right)^{\sum_{\ell=1}^L \zeta_\ell - 1} \Gamma \left(\sum_{\ell=1}^L \zeta_\ell - 1 \right). \quad (34)$$

Employing (31) and (34), we can rewrite I_3 as

$$I_3 = \prod_{\ell=1}^L \frac{s}{\Gamma(m_{s_\ell}) \Gamma(m_\ell)} \left(\frac{1}{2\pi i} \right)^L \int_{\mathcal{L}_1} \int_{\mathcal{L}_2} \dots \int_{\mathcal{L}_L} \frac{\Gamma \left(\sum_{\ell=1}^L \zeta_\ell - 1 \right)}{\Gamma \left(\sum_{\ell=1}^L \zeta_\ell \right)} \prod_{\ell=1}^L \Upsilon(\zeta_\ell) \left(\frac{m_\ell}{s \bar{\gamma}_\ell (m_{s_\ell} - 1)} \right)^{\zeta_\ell} d\zeta_1 d\zeta_2 \dots d\zeta_L. \quad (35)$$

Substituting (35) into (28) and using (6), we obtain (29) which completes the proof. \blacksquare

Remark 2. *With the aid of Theorem 3, a highly accurate approximation of the channel capacity per unit bandwidth under CIFR can be deduced using single \mathcal{F} fading channel. Setting $L = 1$ in (29) and we get the same result as [5, eq. (23)] after some algebraic manipulations. Notice that [5, eq. (23)] is insightful and we can observe that m and m_s have the same influence to the channel capacity under CIFR approximately. Besides, it is easy to see that the channel capacity under CIFR increases as m and m_s increase. Under \mathcal{F} composite fading channel, a high SNR approximation of channel capacity under CIFR was derived as [5, eq. (26)], which can be used as the high-SNR approximation of (29).*

2) *Truncated Channel Inversion with Fixed Rate:* Another approach is to use a modified inversion policy which inverts the channel fading only above a fixed cutoff fade depth. The channel capacity under TIFR policy is defined as

$$C_{\text{TIFR}} = B \log_2 \left(1 + \frac{1}{\int_{z_0}^\infty \frac{f_Z(z)}{z} dz} \right) \int_{z_0}^\infty f_Z(z) dz \quad (36)$$

where z_0 is a cutoff level that can be selected to achieve a specified outage probability or to maximize (36). Notice that (36) reduces to (28) when z_0 approaches zero.

Proposition 4. *The closed-form expression for the capacity under TIFR is given by*

$$C_{\text{TIFR}} = B \log_2 \left(1 + \frac{1}{\frac{1}{z_0} \prod_{\ell=1}^L \frac{1}{\Gamma(m_{s_\ell}) \Gamma(m_\ell)} H_{\text{TIFR}}} \right) \left(1 - \prod_{\ell=1}^L \frac{1}{\Gamma(m_{s_\ell}) \Gamma(m_\ell)} H_{\text{CDF}} \right) \quad (37)$$

where

$$H_{\text{TIFR}} \triangleq H_{2,1:2,1;\dots;2,1}^{0,1:1,2;\dots;1,2} \left(\begin{array}{c} \frac{z_0 m_1}{(m_{s_1}-1)\bar{\gamma}_1} \\ \vdots \\ \frac{z_0 m_L}{(m_{s_L}-1)\bar{\gamma}_L} \end{array} \middle| \begin{array}{c} (0; -1, \dots, -1) : (1, 1), (1 - m_{s_1}, 1); \dots; (1, 1), (1 - m_{s_L}, 1) \\ (-1; -1, \dots, -1) : (m_1, 1); \dots; (m_L, 1) \end{array} \right). \quad (38)$$

Proof: Observe that

$$\int_{z_0}^{\infty} f_Z(z) dz = 1 - \int_0^{z_0} f_Z(z) dz = 1 - F_Z(z_0) \quad (39)$$

where $F_Z(z_0)$ can be deduced using (10). Thus, C_{TIFR} can be expressed as

$$C_{\text{TIFR}} = B \log_2 \left(1 + \frac{1}{\underbrace{\int_{z_0}^{\infty} \frac{f_Z(z)}{z} dz}_{I_5}} \right) \left(1 - \prod_{\ell=1}^L \frac{1}{\Gamma(m_{s_\ell}) \Gamma(m_\ell)} H_{\text{CDF}} \right). \quad (40)$$

Substituting (8) into (40), we can rewrite I_5 as

$$I_5 = \prod_{\ell=1}^L \frac{1}{\Gamma(m_{s_\ell}) \Gamma(m_\ell)} \left(\frac{1}{2\pi i} \right)^L \\ \times \int_{z_0}^{\infty} \int_{\mathcal{L}_1} \int_{\mathcal{L}_2} \dots \int_{\mathcal{L}_L} \frac{1}{\Gamma\left(\sum_{\ell=1}^L \zeta_\ell\right)} \prod_{\ell=1}^L \Upsilon(\zeta_\ell) \left(\frac{m_\ell}{\bar{\gamma}_\ell (m_{s_\ell} - 1)} \right)^{\zeta_\ell} z^{-2 + \sum_{\ell=1}^L \zeta_\ell} d\zeta_1 d\zeta_2 \dots d\zeta_L dz. \quad (41)$$

Note that the order of integration can be interchangeable according to Fubini's theorem, we can express

I_5 as

$$I_5 = \prod_{\ell=1}^L \frac{1}{\Gamma(m_{s_\ell}) \Gamma(m_\ell)} \left(\frac{1}{2\pi i} \right)^L \\ \times \int_{\mathcal{L}_1} \int_{\mathcal{L}_2} \cdots \int_{\mathcal{L}_L} \frac{\Gamma\left(1 - \sum_{\ell=1}^L \zeta_\ell\right)}{\Gamma\left(\sum_{\ell=1}^L \zeta_\ell\right) \Gamma\left(2 - \sum_{\ell=1}^L \zeta_\ell\right)} \prod_{\ell=1}^L \Upsilon(\zeta_\ell) \left(\frac{\gamma_0 m_\ell}{\bar{\gamma}_\ell (m_{s_\ell} - 1)} \right)^{\zeta_\ell} d\zeta_1 d\zeta_2 \cdots d\zeta_L. \quad (42)$$

Employing (6) and substituting (42) into (40), we obtain (37) to complete the proof. \blacksquare

Remark 3. Using Theorem 3, an accurate approximation of the channel capacity under TIFR can be derived by single \mathcal{F} fading channel. Substituting $L = 1$ in (37). After some algebraic manipulations, we can get the same result as [5, eq. (27)] and [5, eq. (28)]. An approximation of channel capacity under TIFR in the high SNR region is given by [5, eq. (30)], which can be used as the high SNR approximation of (37) with the aid of (12). Furthermore, [5, eq. (30)] is particularly insightful because it only has element functions.

3) *Optimal Rate Adaptation with Constant Transmit Power:* The channel capacity under ORA with a constant transmit power is given by [23, eq. (29)]

$$C_{\text{ORA}} = B \int_0^\infty \log_2(1+z) f_Z(z) dz. \quad (43)$$

Proposition 5. Under the ORA scheme, the channel capacity can be expressed as

$$C_{\text{ORA}} = \frac{B}{s \ln(2)} \prod_{\ell=1}^L \frac{1}{\Gamma(m_{s_\ell}) \Gamma(m_\ell)} H_{\text{ORA}} \quad (44)$$

where

$$H_{\text{ORA}} \triangleq H_{4,1;2,1;\dots;2,1;1,2}^{0,3;1,2;\dots;1,2;1,1} \left(\Delta_{\text{ORA}} \left| \begin{array}{l} (0; -1, \dots, -1), (0; -1, \dots, -1), (1; 1, \dots, 1), (2; 1, \dots, 1) : \\ (1; 1, \dots, 1, 0) : \\ (1, 1), (1 - m_{s_1}, 1); \dots; (1, 1), (1 - m_{s_L}, 1); (1, 1) \\ (m_1, 1); \dots; (m_L, 1); (1, 1), (0, 1) \end{array} \right. \right) \quad (45)$$

$$\text{and } \Delta_{\text{ORA}} \triangleq \left(\frac{m_1}{(m_{s_1} - 1)\bar{\gamma}_1}, \dots, \frac{m_L}{(m_{s_L} - 1)\bar{\gamma}_L}, s \right)^T.$$

Proof: Substituting (8) into (43) and changing the order of integration, the channel capacity under

ORA can be expressed as

$$\begin{aligned}
C_{\text{ORA}} = & B \prod_{\ell=1}^L \frac{1}{\Gamma(m_{s_\ell}) \Gamma(m_\ell)} \left(\frac{1}{2\pi i} \right)^L \\
& \times \int_{\mathcal{L}_1} \int_{\mathcal{L}_2} \cdots \int_{\mathcal{L}_L} \frac{1}{\Gamma\left(\sum_{\ell=1}^L \zeta_\ell\right)} \left\{ \prod_{\ell=1}^L \Upsilon(\zeta_\ell) \left(\frac{m_\ell}{\bar{\gamma}_\ell (m_{s_\ell} - 1)} \right)^{\zeta_\ell} \right\} \\
& \times \underbrace{\int_0^\infty \log_2(1+z) z^{-1 + \sum_{\ell=1}^L \zeta_\ell} dz}_{I_6} d\zeta_1 d\zeta_2 \cdots d\zeta_L. \tag{46}
\end{aligned}$$

With the help of [24, eq. 2.6.9.21] and [19, eq. 8.334.3], I_6 can be deduced as

$$I_6 = \int_0^\infty \log_2(1+z) z^{-1 + \sum_{\ell=1}^L \zeta_\ell} d\gamma = -\frac{1}{\ln 2} \Gamma\left(\sum_{\ell=1}^L \zeta_\ell\right) \Gamma\left(-\sum_{\ell=1}^L \zeta_\ell\right) \tag{47}$$

where $-1 < \Re\left(\sum_{\ell=1}^L \zeta_\ell\right) < 0$.

In order to avoid conflicts with the definition of the multivariate H -function, employing [25, eq. 2.5.16], we can express I_6 as

$$I_6 = \frac{1}{\ln(2)} \int_0^\infty G_{2,2}^{1,2} \left(z \left| \begin{array}{c} \sum_{\ell=1}^L \zeta_\ell, \sum_{\ell=1}^L \zeta_\ell \\ \sum_{\ell=1}^L \zeta_\ell, \sum_{\ell=1}^L \zeta_\ell - 1 \end{array} \right. \right) dz, \tag{48}$$

Using [19, eq. (9.301)] and the Laplace transform of Meijers G -function [26, eq. 07.34.22.0003.01], we obtain

$$\begin{aligned}
\mathcal{L} \left\{ G_{2,2}^{1,2} \left(z \left| \begin{array}{c} \sum_{\ell=1}^L \zeta_\ell, \sum_{\ell=1}^L \zeta_\ell \\ \sum_{\ell=1}^L \zeta_\ell, \sum_{\ell=1}^L \zeta_\ell - 1 \end{array} \right. \right) \right\} &= \frac{1}{x} G_{3,2}^{1,3} \left(\frac{1}{x} \left| \begin{array}{c} 0 \sum_{\ell=1}^L \zeta_\ell, \sum_{\ell=1}^L \zeta_\ell \\ \sum_{\ell=1}^L \zeta_\ell, \sum_{\ell=1}^L \zeta_\ell - 1 \end{array} \right. \right) \\
&= \int_{\mathcal{L}_{L+1}} \frac{\Gamma(1 - \zeta_{L+1}) \Gamma^2\left(1 - \sum_{\ell=1}^{L+1} \zeta_\ell\right) \Gamma\left(\sum_{\ell=1}^{L+1} \zeta_\ell\right)}{\Gamma\left(2 - \sum_{\ell=1}^{L+1} \zeta_\ell\right)} x^{\zeta_{L+1}} d\zeta_{L+1}. \tag{49}
\end{aligned}$$

Thus, using the final value theorem and following the similar procedures as the proof of (29), we can

rewrite the channel capacity under ORA as

$$\begin{aligned}
C_{\text{ORA}} &= \frac{B}{s \ln(2)} \prod_{\ell=1}^L \frac{1}{\Gamma(m_{s_\ell}) \Gamma(m_\ell)} \left(\frac{1}{2\pi i} \right)^{L+1} \\
&\times \int_{\mathcal{L}_1} \int_{\mathcal{L}_2} \cdots \int_{\mathcal{L}_{L+1}} \frac{\Gamma^2 \left(1 - \sum_{\ell=1}^{L+1} \zeta_\ell \right) \Gamma \left(\sum_{\ell=1}^{L+1} \zeta_\ell \right)}{\Gamma \left(2 - \sum_{\ell=1}^{L+1} \zeta_\ell \right) \Gamma \left(\sum_{\ell=1}^L \zeta_\ell \right)} \left\{ \prod_{\ell=1}^L \Upsilon(\zeta_\ell) \left(\frac{m_\ell}{\bar{\gamma}_\ell (m_{s_\ell} - 1)} \right)^{\zeta_\ell} \right\} \\
&\times \frac{\Gamma(1 - \zeta_{L+1}) \Gamma(\zeta_{L+1})}{\Gamma(\zeta_{L+1} + 1)} s^{\zeta_{L+1}} d\zeta_1 d\zeta_2 \cdots d\zeta_{L+1}. \tag{50}
\end{aligned}$$

Equation (44) is obtained using (50) and (6), which completes the proof. \blacksquare

Remark 4. *With the help of Theorem 3, channel capacity under ORA has a tight approximation which can be derived using single \mathcal{F} fading channel. Substituting (47) into (46) and letting $L = 1$, we get the same result as [5, eq. (19)]. An approximation of [5, eq. (19)] in the high SNR region is given by [18, eq. (26)]. Using (12), we get a simple algebraic representation of the approximation of channel capacity under ORA in the high SNR region as [18, eq. (26)], which also provides useful insights on the impact of the involved parameters. For example, it is evident [18, eq. (26)] can be expressed in terms of $\bar{\gamma}_{\mathcal{F}}$. This transformation is useful in quantifying the average SNR value under different fading conditions.*

4) *Optimal Power and Rate Adaptation:* Under OPRA, the channel capacity is given by [27, eq. (7)]

$$C_{\text{OPRA}} = B \int_{\gamma_0}^{\infty} \log_2 \left(\frac{z}{\gamma_0} \right) f_Z(z) dz \tag{51}$$

where γ_0 is the cutoff carrier-to-noise ratio value. No data is sent below γ_0 and γ_0 must satisfy [27, eq. (6)]

$$\int_{\gamma_0}^{\infty} \left(\frac{1}{\gamma_0} - \frac{1}{z} \right) f_Z(z) dz = 1. \tag{52}$$

Let

$$S(z) = \begin{cases} \frac{1}{\gamma_0} - \frac{1}{z} & z \geq \gamma_0, \\ 0 & \text{otherwise,} \end{cases} \tag{53}$$

the channel capacity under OPRA can also be written as

$$C_{\text{OPRA}} = B \int_0^{\infty} \log_2(1 + S(z)z) f_Z(z) dz. \tag{54}$$

Proposition 6. *The channel capacity under OPRA is derived as*

$$C_{\text{OPRA}} = \prod_{\ell=1}^L \frac{1}{\Gamma(m_\ell) \Gamma(m_{s_\ell})} H_{\text{OPRA}} \quad (55)$$

where

$$H_{\text{OPRA}} \triangleq H_{4,1:2,1;\dots;2,1;0,1}^{0,2:1,2;\dots;1,2;1,0} \left(\Delta_{\text{OPRA}} \left| \begin{array}{l} (1; -1, \dots, -1), (1; -1, \dots, -1), (1; 1, \dots, 1), (1; 1, \dots, 1) : \\ (1; 1, \dots, 1) : \\ (1, 1), (1 - m_{s_1}, 1); \dots; (1, 1), (1 - m_{s_L}, 1); - \\ (m_1, 1); \dots; (m_L, 1); (0, 1) \end{array} \right. \right) \quad (56)$$

$$\text{and } \Delta_{\text{OPRA}} \triangleq \left(\frac{\gamma_0 m_1}{(m_{s_1} - 1) \bar{\gamma}_1}, \dots, \frac{\gamma_0 m_L}{(m_{s_L} - 1) \bar{\gamma}_L}, s \right)^T.$$

Proof: Substituting (8) into (51) and changing the order of integration, we can rewrite the channel capacity under OPRA as

$$C_{\text{OPRA}} = \prod_{\ell=1}^L \frac{1}{\Gamma(m_\ell) \Gamma(m_{s_\ell})} \left(\frac{1}{2\pi i} \right)^L \int_{\mathcal{L}_1} \int_{\mathcal{L}_2} \dots \int_{\mathcal{L}_L} \frac{1}{\Gamma\left(\sum_{\ell=1}^L \zeta_\ell\right)} \prod_{\ell=1}^L \Upsilon(\zeta_\ell) \left(\frac{m_\ell}{\bar{\gamma}_\ell (m_{s_\ell} - 1)} \right)^{\zeta_\ell} \\ \times \underbrace{\int_{\gamma_0}^{\infty} \log_2 \left(\frac{z}{\gamma_0} \right) z^{-1 + \sum_{\ell=1}^L \zeta_\ell} dz}_{I_7} d\zeta_1 d\zeta_2 \dots d\zeta_L. \quad (57)$$

Let $t = z/\gamma_0 - 1$ and we have

$$I_7 = \gamma_0^{\sum_{\ell=1}^L \zeta_\ell} \int_0^{\infty} \log_2(t+1) (t+1)^{-1 + \sum_{\ell=1}^L \zeta_\ell} dt. \quad (58)$$

Using [24, eq. (2.6.10.49)], [24, eq. (II.2)] and [19, eq. (8.331.1)], we can solve I_7 as

$$I_7 = \frac{1}{\ln 2} \frac{\Gamma\left(-\sum_{\ell=1}^L \zeta_\ell\right) \Gamma\left(-\sum_{\ell=1}^L \zeta_\ell\right) \gamma_0^{\sum_{\ell=1}^L \zeta_\ell}}{\Gamma\left(1 - \sum_{\ell=1}^L \zeta_\ell\right) \Gamma\left(1 - \sum_{\ell=1}^L \zeta_\ell\right)}. \quad (59)$$

However, eq. (59) has conflict with the definition of the multivariate Fox's H -function, so we choose another way to solve I_7 . Using the final value theorem and following the similar procedures as the proof

of (29), we can rewrite I_7 as

$$I_7 = \frac{1}{2\pi j} \gamma_0^{\sum_{\ell=1}^L \zeta_\ell} \int_{\mathcal{L}_{L+1}} \frac{\Gamma^2 \left(-\sum_{\ell=1}^{L+1} \zeta_\ell \right) \Gamma(-\zeta_{L+1})}{\Gamma^2 \left(1 - \sum_{\ell=1}^{L+1} \zeta_\ell \right)} s^{\zeta_{L+1}} d\zeta_{L+1}. \quad (60)$$

Substituting (60) into (57), we obtain

$$\begin{aligned} C_{\text{OPRA}} &= \prod_{\ell=1}^L \frac{1}{\Gamma(m_\ell) \Gamma(m_{s_\ell})} \left(\frac{1}{2\pi i} \right)^{L+1} \int_{\mathcal{L}_1} \int_{\mathcal{L}_2} \cdots \int_{\mathcal{L}_{L+1}} \frac{\Gamma^2 \left(-\sum_{\ell=1}^{L+1} \zeta_\ell \right)}{\Gamma \left(\sum_{\ell=1}^L \zeta_\ell \right) \Gamma^2 \left(1 - \sum_{\ell=1}^{L+1} \zeta_\ell \right)} \\ &\quad \times \prod_{\ell=1}^L \Upsilon(\zeta_\ell) \left(\frac{\gamma_0 m_\ell}{\bar{\gamma}_\ell (m_{s_\ell} - 1)} \right)^{\zeta_\ell} \Gamma(-\zeta_{L+1}) s^{\zeta_{L+1}} d\zeta_1 d\zeta_2 \cdots d\zeta_{L+1}. \end{aligned} \quad (61)$$

With the help of (6), we obtain (55). The proof is now complete. \blacksquare

Remark 5. Based on Theorem 3, A tight approximation of channel capacity under OPRA can be derived using single \mathcal{F} fading channel. Substituting (59) into (57) and letting $L = 1$, the same result as [18, eq. (52)] is obtained as Note that [18, eq. (52)] is suitable for analysis both analytically and numerically and can be used as a benchmark for further derivation of an approximation. In the high-SNR regime, the approximation of (55) is given as [18, eq. (57)].

Remark 6. In order to determine the value of γ_0 , we can rewrite (52) as

$$\frac{1}{\gamma_0} \underbrace{\int_{\gamma_0}^{\infty} f_Z(z) dz}_{I_8} - \underbrace{\int_{\gamma_0}^{\infty} \frac{f_Z(z)}{z} dz}_{I_9} = 0 \quad (62)$$

where I_8 and I_9 have been solved in (39) and (42) respectively. Thus, it follows that

$$\frac{1}{\gamma_0} \left(1 - \prod_{\ell=1}^L \frac{1}{\Gamma(m_{s_\ell}) \Gamma(m_\ell)} H_{\text{CDF}} \right) - \prod_{\ell=1}^L \frac{1}{\Gamma(m_{s_\ell}) \Gamma(m_\ell)} H_{\text{TIFR}} = 0. \quad (63)$$

A detailed proof of the existence of γ_0 in the range $[0, 1]$ is given in [28]. Thus, with the aid of (63), γ_0 can be solved with mathematical software and we find that using the dichotomy for iterations within 20 times can make the error less than 10^{-6} .

Remark 7. Channel capacity in AWGN, in bits per second, is given by Shannons formula as [29]

$$C_{\text{AWGN}} = B \log_2(1 + z). \quad (64)$$

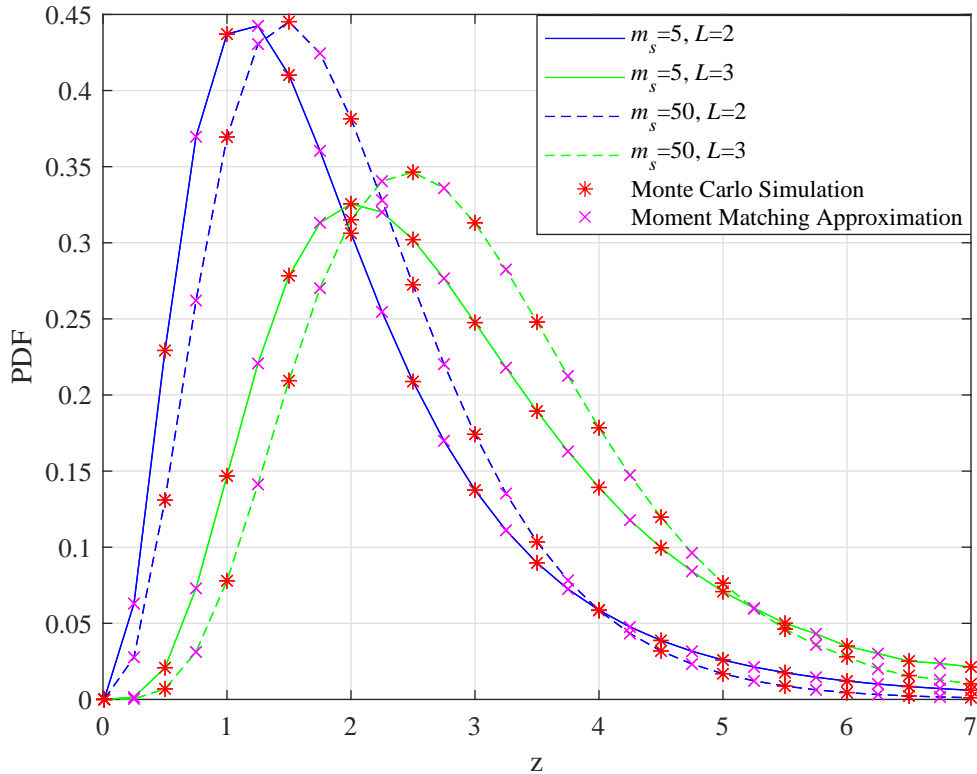


Fig. 3. PDF for the sum of squared \mathcal{F} -distributed RVs.

The relationship of C_{ORA} , C_{OPRA} and C_{AWGN} can be obtained by applying the Jensen's inequality as [30]

$$0 \leq C_{\text{OPRA}} - C_{\text{ORA}} \leq \min(C_{\text{OPRA}}, -\log_2 \gamma_0) \quad (65a)$$

$$C_{\text{ORA}} \leq C_{\text{AWGN}} \quad (65b)$$

and there is no general order relation between C_{OPRA} and C_{AWGN} .

VI. NUMERICAL RESULTS

In this section, analytical results are presented to illustrate the proposed applications of the sum of Fisher-Snedecor \mathcal{F} RVs in wireless communication systems. All results are substantiated by Monte Carlo simulations.

Figures 3 and 4, respectively, plot the PDF and CDF of the sum of Fisher-Snedecor \mathcal{F} RVs and their proposed approximation obtained by moment matching method for different values of m_s and L , assuming $m_{s_\ell} = m_s$ ($\ell = 1, 2, 3$), $m_\ell = 2$, $\gamma_\ell = 0$ dB. In both figures, it can be observed that the approximate PDFs

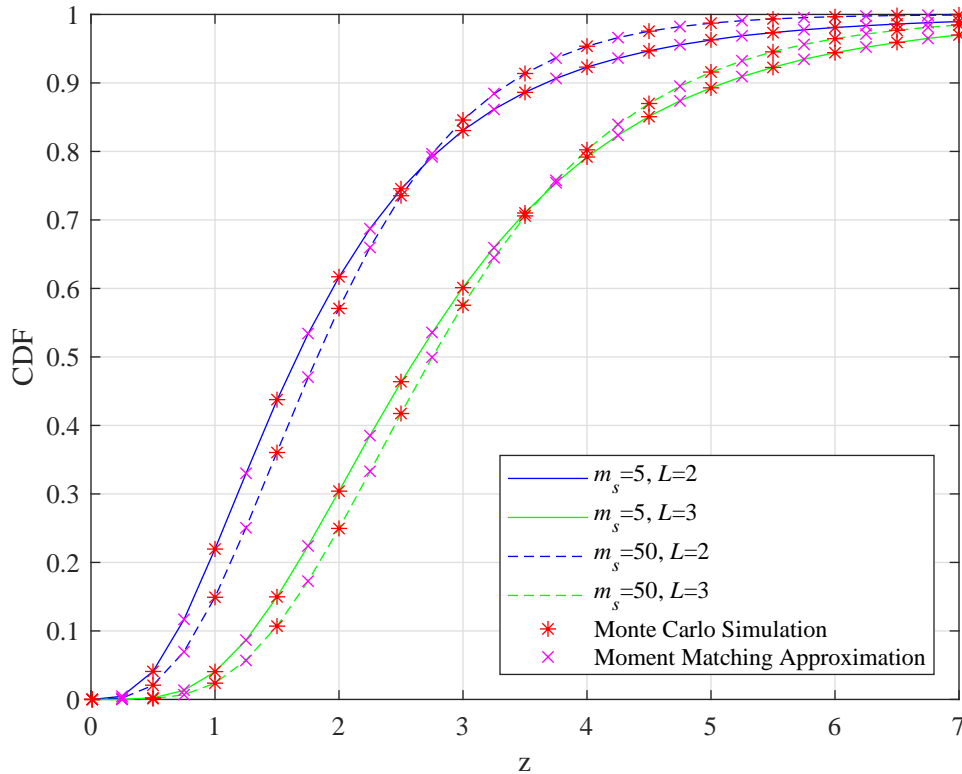


Fig. 4. CDF for the sum of squared \mathcal{F} -distributed RVs.

and CDFs match the exact ones well for all considered cases. Furthermore, analytical results perfectly match Monte Carlo simulations, thus validating our results.

Figure 5 depicts the OP performance versus average SNR γ for a dual-, triple- and quadruple-branch MRC receivers with $\gamma_\ell = \gamma$ ($\ell = 1, 2, 3, 4$), $\gamma_{\text{th}} = 0$ dB, $m_\ell = 1.5$, $m_{s_\ell} = 5$. As it can be observed, the OP decreases as the average SNR and L increase. Again, it is evident that the exact results match the approximate ones and Monte Carlo simulations well. In addition, the asymptotic expressions match well the exact ones at high-SNR values thus proving their validity and versatility. The OP performance improvement is more pronounced by increasing $L = 2$ to $L = 3$.

Figures 6-9, respectively, show the analytical and simulated channel capacities versus average SNR γ under different adaptive transmission strategies respectively, assuming $L = 2$. Figs. 6 and 7 illustrate the channel capacity increases as m increases, while Figs. 8 and 9 depict the channel capacity increases as m_s increases, which means favorable system parameters can lead to a large channel capacity. Once again, perfect agreement is observed between analytical results, approximate results and Monte Carlo simulations in Figs. 6-9.

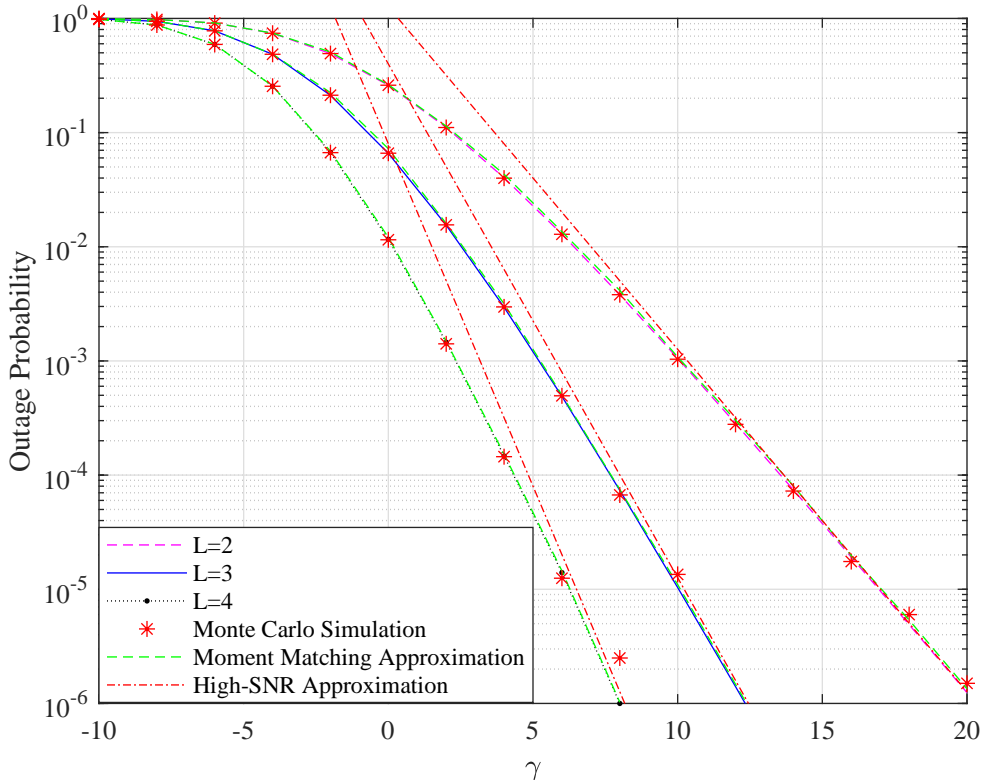


Fig. 5. Outage probability versus average SNR for dual, triple and quadruple MRC receivers.

As shown in Fig. 10, four different adaptive transmission strategies provide different channel capacities. Obviously, the relation we proposed in (7) is shown. As it can be observed, the channel capacity under OPRA is the largest among those adaptive transmission strategies, followed by the channel capacity under ORA. The channel capacity under TIFR and CIFR converges in the high-SNR regime because the asymptotic expressions of those two cases are the same for $m > 1$. This finding can be also observed in channel capacity under OPRA and ORA. Moreover, analytical and approximate results agree well with Monte Carlo simulations.

Figure 11 illustrates the effective capacity of MRC systems over i.n.i.d. \mathcal{F} fading channels as a function of the delay constraint A for different settings of the parameters m_s and L , assuming $m_{s_\ell} = m_s$, $m_\ell = 5$, $\gamma_\ell = 10$ dB ($\ell = 1, 2, 3$). It can be easily observed that, the effective capacity increases as m_s and L increase. This is because of the fact that large value of m_s induces low shadowing effect and large value of L means more receive power. For a certain setting of the parameters, the effective capacity increases as A decreases (i.e. large delay). Thus, the considered system can support larger arrival rates with a larger delay constraint. Fig. 11 shows a perfect agreement of the Monte Carlo simulations and analytical and

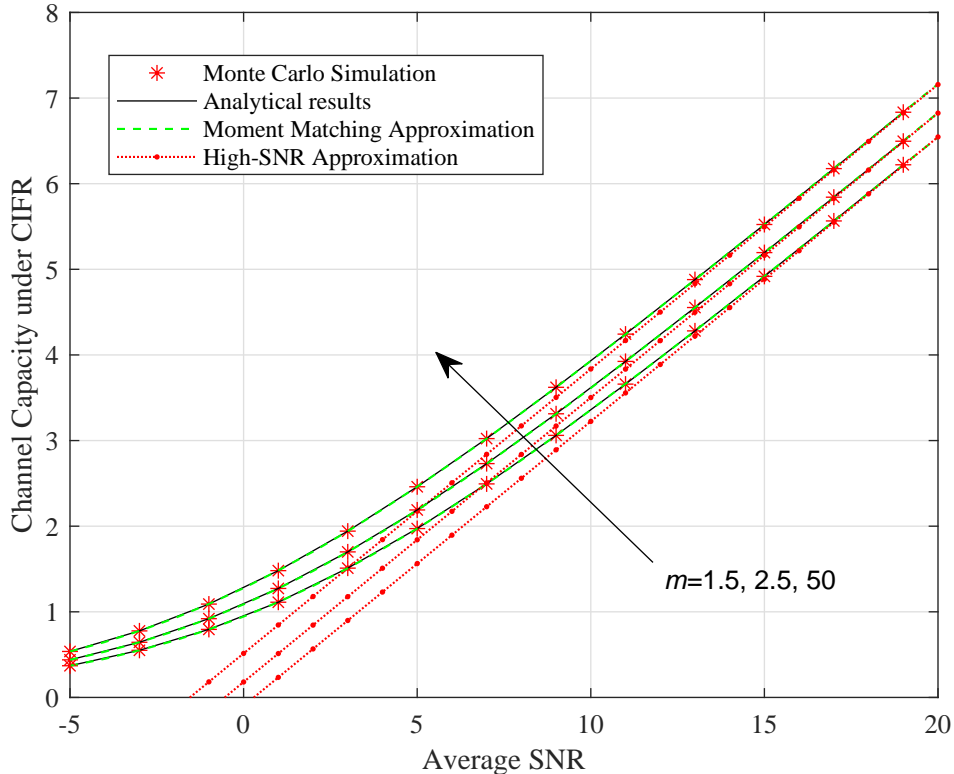


Fig. 6. Channel capacity under CIFR versus average SNR for $L=2$.

simulation results, which confirms the validity of the analytical result in (22).

VII. CONCLUSION

We presented exact expressions for the PDF and CDF of i.n.i.d. Fisher-Snedecor \mathcal{F} RVs. In addition, we proposed the single \mathcal{F} distribution with an adjusted form of parameters to approximate the sum of \mathcal{F} distribution by using the moment matching method. The derived results show that the introduced adjustment results closely approximate in both the lower and upper tail regions. This sufficiently accurate region-wise approximation significantly simplify the performance analysis of MRC diversity receivers over \mathcal{F} fading channels. To this end, novel, computationally efficient analytical expressions were obtained for OP, effective capacity and channel capacities under different adaptive transmission strategies. Finally, Extensive numerical results have been presented to validate the proposed analytical expressions and an excellent agreement has been observed. The new and important insights we provided are useful for wireless communication system designers.

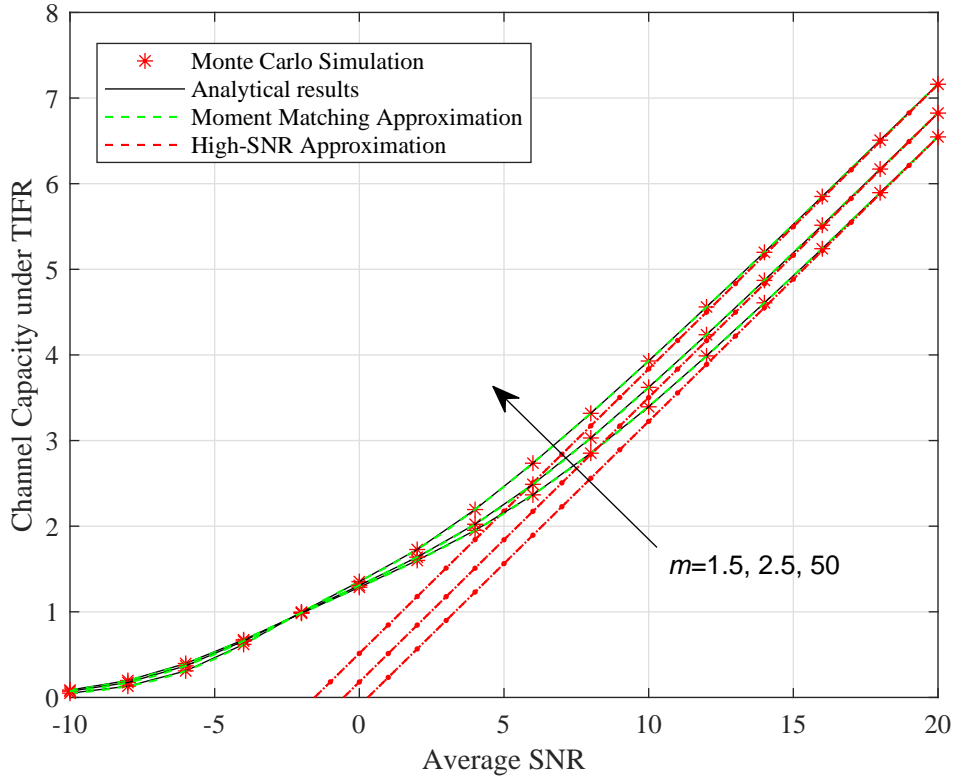


Fig. 7. Channel capacity under TIFR versus average SNR for $L=2$.

APPENDIX A

PROOF OF THEOREM 1

The PDF of z can be obtained as

$$f_z(z) = \mathcal{L}^{-1}\{\mathcal{M}_z(s); z\} = \frac{1}{2\pi j} \int_{\mathcal{L}} \mathcal{M}_z(s) e^{zs} ds \quad (\text{A-1})$$

where $\mathcal{L}^{-1}\{\cdot\}$ denotes the inverse Laplace transform and $\mathcal{M}_z(s)$ is the MGF of z . Because the Fisher-Snedecor \mathcal{F} RVs are independent, we can obtain the MGF of the z using (4) as

$$\mathcal{M}_z(s) = \prod_{\ell=1}^L \mathcal{M}_{\gamma_{\ell}}(s) = \prod_{\ell=1}^L \frac{\Gamma(m_{\ell} + m_{s_{\ell}})}{\Gamma(m_{s_{\ell}})} \Psi\left(m_{\ell}; 1 - m_{s_{\ell}}; \frac{s\bar{\gamma}_{\ell}(m_{s_{\ell}} - 1)}{m_{\ell}}\right). \quad (\text{A-2})$$

Substituting (A-2) into (A-1) and using [31, eq. (8.4.46.1)], we can derive the MGF of z as

$$f_z(z) = \frac{1}{2\pi j} \int_{\mathcal{L}} \prod_{\ell=1}^L \frac{1}{\Gamma(m_{s_{\ell}}) \Gamma(m_{\ell})} G_{1,2}^{2,1}\left(\frac{s\bar{\gamma}_{\ell}(m_{s_{\ell}} - 1)}{m_{\ell}} \middle| \begin{matrix} 1 - m_{\ell} \\ 0, m_{s_{\ell}} \end{matrix}\right) e^{zs} ds \quad (\text{A-3})$$

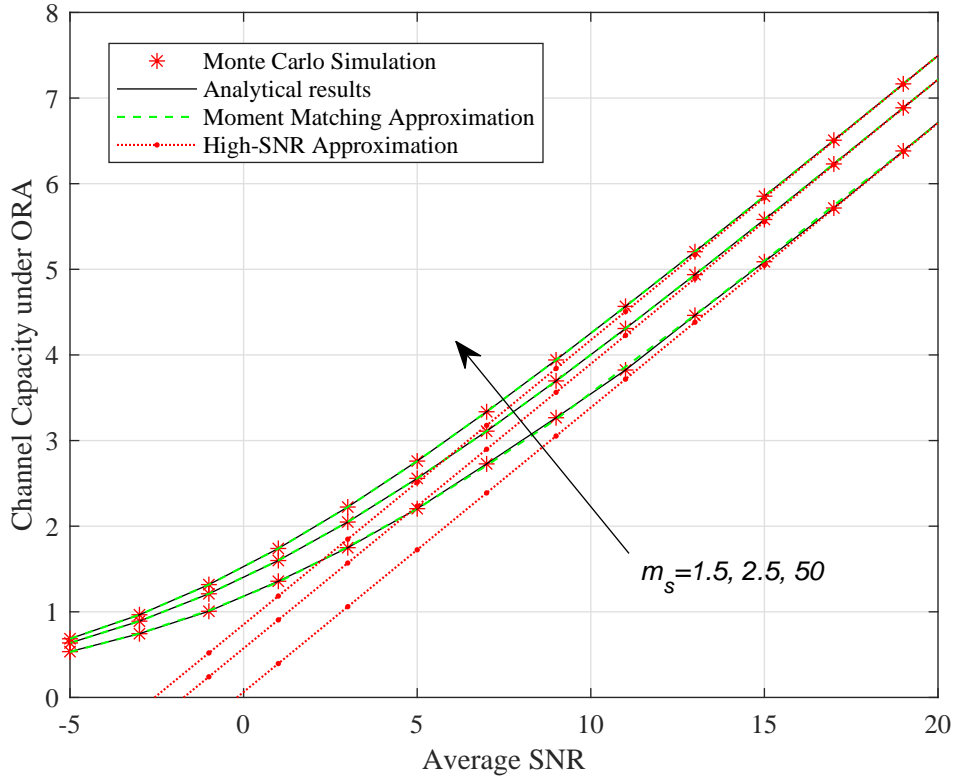


Fig. 8. Channel capacity under ORA versus average SNR for $L=2$.

where the integration path of \mathcal{L} goes from $\sigma - \infty j$ to $\sigma + \infty j$ and $\sigma \in \mathbb{R}$. Rewriting each Meijers G -function as a Mellin-Barnes integral with the aid of [19, eq. (8.4.3.1)] and merging the integrals, we obtain

$$\begin{aligned}
 f_z(z) &= \prod_{\ell=1}^L \frac{1}{\Gamma(m_{s_\ell}) \Gamma(m_\ell)} \int_{\mathcal{L}_1} \int_{\mathcal{L}_2} \cdots \int_{\mathcal{L}_L} \left(\frac{1}{2\pi j} \right)^L \prod_{\ell=1}^L \Gamma(-t_\ell) \Gamma(m_\ell + t_\ell) \Gamma(m_\ell + m_{s_\ell} + t_\ell) \\
 &\quad \times \left(\frac{\bar{\gamma}_\ell (m_{s_\ell} - 1)}{m_\ell} \right)^{-(m_\ell + t_\ell)} \underbrace{\frac{1}{2\pi j} \int_{\mathcal{L}} s^{-\sum_{\ell=1}^L m_\ell - \sum_{\ell=1}^L t_\ell} e^{zs} ds dt_1 dt_2 \cdots dt_L}_{I_A}
 \end{aligned} \tag{A-4}$$

where \mathcal{L}_ℓ ($\ell = 1, \dots, L$), goes from $\sigma_\ell - \infty j$ to $\sigma_\ell + \infty j$ and $\sigma_\ell \in \mathbb{R}$. Using [19, eq. (8.315.1)], we can solve I_A as

$$I_A = z^{-1 + \sum_{\ell=1}^L m_\ell + \sum_{\ell=1}^L t_\ell} \frac{1}{\Gamma\left(\sum_{\ell=1}^L m_\ell + \sum_{\ell=1}^L t_\ell\right)}. \tag{A-5}$$

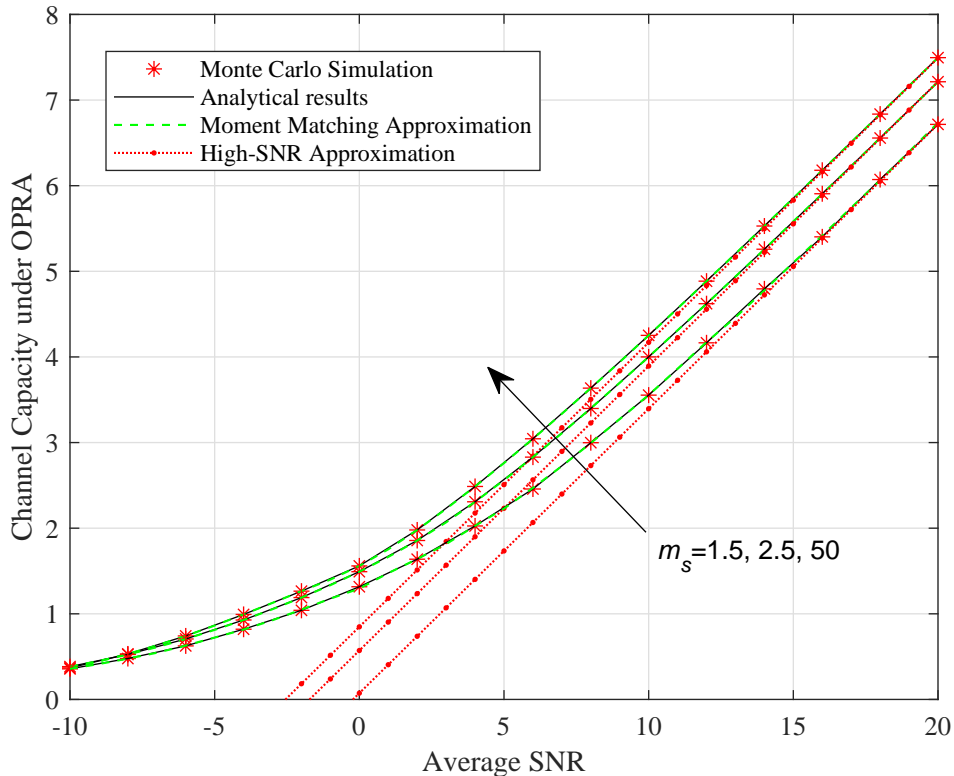


Fig. 9. Channel capacity under OPRA versus average SNR for $L=2$.

Let $\zeta_\ell \triangleq m_\ell + t_\ell$. Substitute (A-5) into (A-4), we can write (A-4) as

$$\begin{aligned}
 f_z(z) &= \frac{1}{z} \prod_{\ell=1}^L \frac{1}{\Gamma(m_{s_\ell}) \Gamma(m_\ell)} \int_{\mathcal{L}_1} \int_{\mathcal{L}_2} \cdots \int_{\mathcal{L}_L} \left(\frac{1}{2\pi j} \right)^L \frac{1}{\Gamma\left(\sum_{\ell=1}^L \zeta_\ell\right)} \\
 &\quad \times \prod_{\ell=1}^L \Gamma(m_\ell - \zeta_\ell) \Gamma(\zeta_\ell) \Gamma(m_{s_\ell} + \zeta_\ell) \left(\frac{z m_\ell}{\bar{\gamma}_\ell (m_{s_\ell} - 1)} \right)^{\zeta_\ell} d\zeta_1 d\zeta_2 \cdots d\zeta_L. \quad (\text{A-6})
 \end{aligned}$$

The proof is completed by deriving (8) with the definition of the multivariate H -function [20, eq. (A.1)].

APPENDIX B

PROOF OF THEOREM 3

Let us start with $L = 2$ and $z = \gamma_1 + \gamma_2$, $z \sim \mathcal{F}(\bar{\gamma}, m, m_s)$ and $\gamma_\ell \sim \mathcal{F}(\bar{\gamma}_\ell, m_\ell, m_{s_\ell})$ ($\ell = 1, 2$). The first, second and third moments of the sum of two independent RVs can be written as

$$\begin{cases}
 \text{E}[z] = \text{E}[\gamma_1] + \text{E}[\gamma_2], \\
 \text{E}[z^2] = \text{E}[\gamma_1^2] + \text{E}[\gamma_2^2] + 2\text{E}[\gamma_1] \text{E}[\gamma_2], \\
 \text{E}[z^3] = \text{E}[\gamma_1^3] + \text{E}[\gamma_2^3] + 3\text{E}[\gamma_1^2] \text{E}[\gamma_2] + 3\text{E}[\gamma_1] \text{E}[\gamma_2^2],
 \end{cases} \quad (\text{B-1})$$

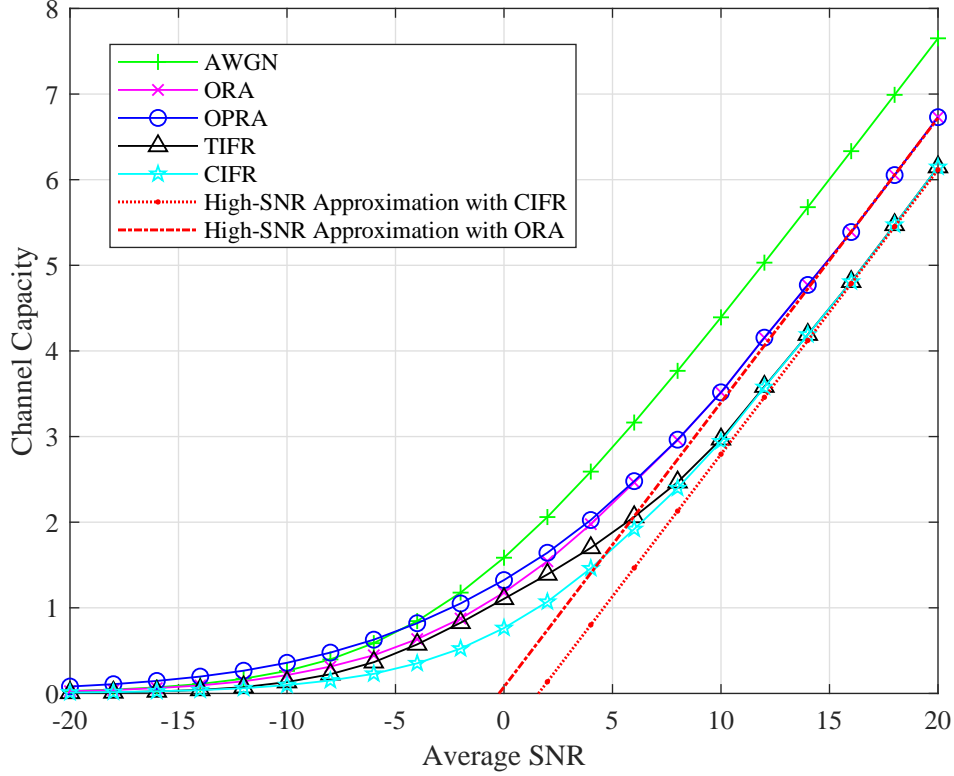


Fig. 10. Channel capacity under four different adaptive transmission strategies versus average SNR for $L=2$.

With the help of (5), eq. (B-1) can be written as

$$\begin{cases} \bar{\gamma}_{\mathcal{F}} = \bar{\gamma}_1 + \bar{\gamma}_2, \\ H_{\mathcal{F}} \bar{\gamma}^2 = H_1 \bar{\gamma}_1^2 + H_2 \bar{\gamma}_2^2 + 2\bar{\gamma}_1 \bar{\gamma}_2, \\ H_{\mathcal{F}} Y_{\mathcal{F}} \bar{\gamma}^3 = H_1 Y_1 \bar{\gamma}_1^3 + H_2 Y_2 \bar{\gamma}_2^3 + 3H_1 \bar{\gamma}_1^2 \bar{\gamma}_2 + 3H_2 \bar{\gamma}_1 \bar{\gamma}_2^2 \end{cases} \quad (\text{B-2})$$

where $H_{\mathcal{F}} = \frac{(1+m)(m_s-1)}{m(m_s-2)}$, $Y_{\mathcal{F}} = \frac{(m_s-1)(2+m)}{m(m_s-3)}$, $H_{\ell} = \frac{(1+m_{\ell})(m_{s_{\ell}}-1)}{m_{\ell}(m_{s_{\ell}}-2)}$, $Y_{\ell} = \frac{(m_{s_{\ell}}-1)(2+m_{\ell})}{m_{\ell}(m_{s_{\ell}}-3)}$ ($\ell = 1, 2$). In the composite fading channel, an \mathcal{F} fading channel's amount of fading (AF), which is often used as a relative measure of the severity of fading, is derived in [1] as $(H_{\mathcal{F}} - 1)$. By solving (B-2), we obtain

$$\begin{cases} \bar{\gamma}_{\mathcal{F}} = \bar{\gamma}_1 + \bar{\gamma}_2, \\ H_{\mathcal{F}} = \frac{H_1 \bar{\gamma}_1^2 + H_2 \bar{\gamma}_2^2 + 2\bar{\gamma}_1 \bar{\gamma}_2}{(\bar{\gamma}_1 + \bar{\gamma}_2)^2} = \frac{(H_1 - 1)\bar{\gamma}_1^2 + (H_2 - 1)\bar{\gamma}_2^2}{(\bar{\gamma}_1 + \bar{\gamma}_2)^2} + 1, \\ Y_{\mathcal{F}} = \frac{H_1 Y_1 \bar{\gamma}_1^3 + H_2 Y_2 \bar{\gamma}_2^3 + 3\bar{\gamma}_1^2 \bar{\gamma}_2 H_1 + 3\bar{\gamma}_1 \bar{\gamma}_2^2 H_2}{(\bar{\gamma}_1 + \bar{\gamma}_2)(H_1 \bar{\gamma}_1^2 + H_2 \bar{\gamma}_2^2 + 2\bar{\gamma}_1 \bar{\gamma}_2)} \\ = \frac{(H_1 Y_1 - 1)\bar{\gamma}_1^3 + (H_2 Y_2 - 1)\bar{\gamma}_2^3 + (\bar{\gamma}_1 + \bar{\gamma}_2)^3 + 3(\bar{\gamma}_1 + \bar{\gamma}_2)(\bar{\gamma}_1^2(H_1 - 1) + \bar{\gamma}_2^2(H_2 - 1)) - 3(\bar{\gamma}_1^3(H_1 - 1) + \bar{\gamma}_2^3(H_2 - 1))}{(\bar{\gamma}_1 + \bar{\gamma}_2)((H_1 - 1)\bar{\gamma}_1^2 + (H_2 - 1)\bar{\gamma}_2^2 + (\bar{\gamma}_1 + \bar{\gamma}_2)^2)}. \end{cases} \quad (\text{B-3})$$

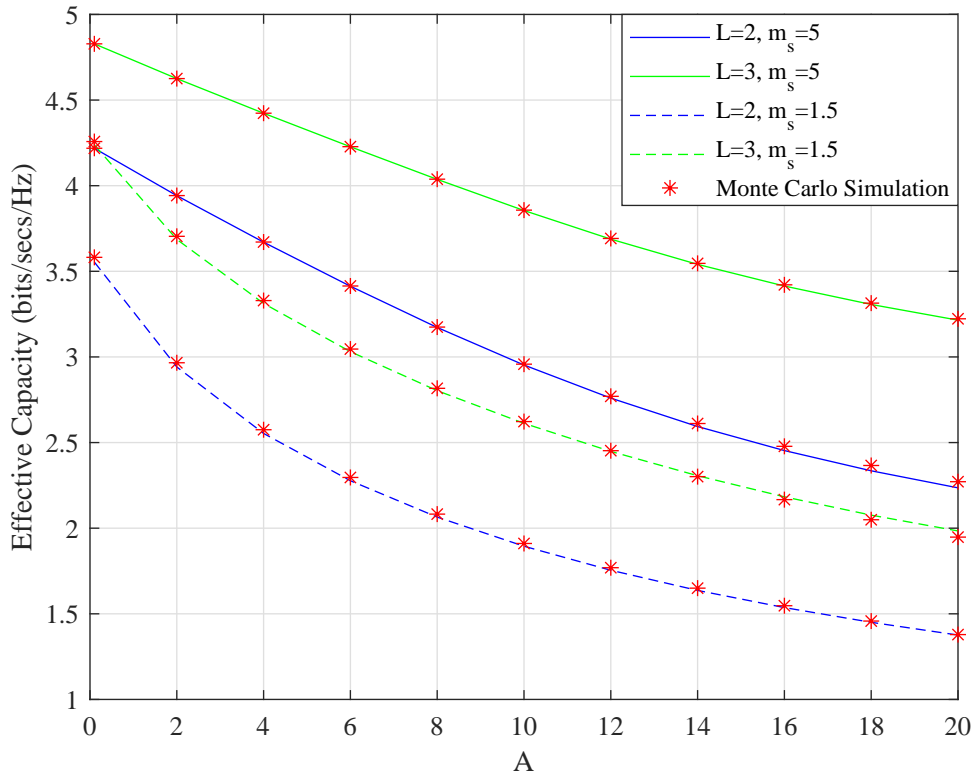


Fig. 11. Effective capacity of MRC receivers over i.n.i.d. \mathcal{F} fading channels versus the delay constraint A .

Equations (B-3) can be generalized for the sum of L i.n.i.d. Fisher-Snedecor \mathcal{F} RVs as [32]

$$\left\{ \begin{array}{l} \bar{\gamma}_{\mathcal{F}} = \sum_{\ell=1}^L \bar{\gamma}_{\ell}, \\ H_{\mathcal{F}} = \frac{\sum_{\ell=1}^L (H_{\ell}-1)\bar{\gamma}_{\ell}^2}{\left(\sum_{\ell=1}^L \bar{\gamma}_{\ell}\right)^2} + 1, \\ Y_{\mathcal{F}} = \frac{\sum_{\ell=1}^L (H_{\ell}Y_{\ell}-1)\bar{\gamma}_{\ell}^3 + \left(\sum_{\ell=1}^L \bar{\gamma}_{\ell}\right)^3 + 3\left(\sum_{\ell=1}^L \bar{\gamma}_{\ell}\right)\left(\sum_{\ell=1}^L (H_{\ell}-1)\bar{\gamma}_{\ell}^2\right) - 3\sum_{\ell=1}^L (H_{\ell}-1)\bar{\gamma}_{\ell}^3}{\left(\sum_{\ell=1}^L \bar{\gamma}_{\ell}\right)\left(\sum_{\ell=1}^L (H_{\ell}-1)\bar{\gamma}_{\ell}^2 + \left(\sum_{\ell=1}^L \bar{\gamma}_{\ell}\right)^2\right)}. \end{array} \right. \quad (\text{B-4})$$

However, the parameters of a single \mathcal{F} distribution calculated by (B-4) result in a relatively large approximation error in the lower and upper tail regions because we only match the first, second and third moments. This error can be modified by introducing an adjustment factor ε . The proof is complete by deriving (12) and (13).

REFERENCES

- [1] S. K. Yoo, S. L. Cotton, P. C. Sofotasios, M. Matthaiou, M. Valkama, and G. K. Karagiannidis, "The Fisher-Snedecor \mathcal{F} distribution: A simple and accurate composite fading model," *IEEE Commun. Lett.*, vol. 21, no. 7, pp. 1661–1664, Jul. 2017.
- [2] L. Kong and G. Kaddoum, "On physical layer security over the Fisher-Snedecor \mathcal{F} wiretap fading channels," *IEEE Access*, vol. 6, pp. 39 466–39 472, Jul. 2018.
- [3] N. Kapucu and M. Bilim, "Analysis of analytical capacity for Fisher-Snedecor \mathcal{F} fading channels with different transmission schemes," *Electron. Lett.*, vol. 55, no. 5, pp. 283–285, May 2019.
- [4] S. K. Yoo, P. C. Sofotasios, S. L. Cotton, S. Muhaidat, O. S. Badarneh, and G. K. Karagiannidis, "Entropy and energy detection-based spectrum sensing over \mathcal{F} composite fading channels," *IEEE Trans. Commun.*, vol. 67, no. 7, pp. 4641–4653, Jul. 2019.
- [5] H. Zhao, L. Yang, A. S. Salem, and M.-S. Alouini, "Ergodic capacity under power adaption over Fisher-Snedecor \mathcal{F} fading channels," *IEEE Commun. Lett.*, vol. 23, no. 3, pp. 546–549, Mar. 2019.
- [6] M. K. Simon and M.-S. Alouini, *Digital Communication Over Fading Channels*. John Wiley & Sons, 2005.
- [7] S. Chen, J. Zhang, G. K. Karagiannidis, and B. Ai, "Effective rate of MISO systems over Fisher-Snedecor \mathcal{F} fading channels," *IEEE Commun. Lett.*, vol. 22, no. 12, pp. 2619–2622, Dec. 2018.
- [8] F. El Bouanani and D. B. da Costa, "Accurate closed-form approximations for the sum of correlated weibull random variables," *IEEE Wireless Commun. Lett.*, vol. 7, no. 4, pp. 498–501, Aug. 2018.
- [9] J. Zhang, L. Dai, Y. Han, Y. Zhang, and Z. Wang, "On the ergodic capacity of MIMO free-space optical systems over turbulence channels," *IEEE J. Sel. Areas in Commun.*, vol. 33, no. 9, pp. 1925–1934, Sep. 2015.
- [10] J. Zhang, M. Matthaiou, G. K. Karagiannidis, and L. Dai, "On the multivariate Gamma-Gamma distribution with arbitrary correlation and applications in wireless communications," *IEEE Trans. Veh. Technol.*, vol. 65, no. 5, pp. 3834–3840, May 2015.
- [11] K. Peppas, F. Lazarakis, A. Alexandridis, and K. Dangakis, "Error performance of digital modulation schemes with MRC diversity reception over η - μ fading channels," *IEEE Trans. Wireless Commun.*, vol. 8, no. 10, pp. 4974–4980, Oct. 2009.
- [12] J. Zheng, J. Zhang, G. Pan, J. Cheng, and B. Ai, "Sum of squared fluctuating two-ray random variables with wireless applications," *IEEE Trans. Veh. Technol.*, vol. 68, no. 8, pp. 8173–8177, Aug. 2019.
- [13] O. S. Badarneh, D. B. da Costa, P. C. Sofotasios, S. Muhaidat, and S. L. Cotton, "On the sum of Fisher-Snedecor \mathcal{F} variates and its application to maximal-ratio combining," *IEEE Wireless Commun. Lett.*, vol. 7, no. 6, pp. 966–969, Dec. 2018.
- [14] J. Sánchez, D. Osorio, E. Olivo, H. Alves, M. C. P. Paredes, and L. Urquiza-Aguiar, "On the statistics of the ratio of non-constrained arbitrary α - μ random variables: a general framework and applications," *arXiv:1902.07847*, Feb. 2019.
- [15] C. R. N. Da Silva, N. Simmons, E. J. Leonardo, S. L. Cotton, and M. D. Yacoub, "Ratio of two envelopes taken from $\alpha - \mu$, $\eta - \mu$, and $\kappa - \mu$ variates and some practical applications," *IEEE Access*, vol. 7, pp. 54 449–54 463, May 2019.
- [16] H. R. Alhennawi, M. M. El Ayadi, M. H. Ismail, and H.-A. M. Mourad, "Closed-form exact and asymptotic expressions for the symbol error rate and capacity of the H-function fading channel," *IEEE Trans. Veh. Technol.*, vol. 65, no. 4, pp. 1957–1974, Apr. 2015.
- [17] H. Chergui, M. Benjillali, and M.-S. Alouini, "Rician K -factor-based analysis of XLOS service probability in 5G outdoor ultra-dense networks," *IEEE Wireless Commun. Lett.*, vol. 8, no. 2, pp. 428–431, Apr. 2018.
- [18] S. K. Yoo, P. C. Sofotasios, S. L. Cotton, S. Muhaidat, F. J. Lopez-Martinez, J. M. Romero-Jerez, and G. K. Karagiannidis, "A comprehensive analysis of the achievable channel capacity in \mathcal{F} composite fading channels," *IEEE Access*, vol. 7, pp. 34 078 –34 094, Mar. 2019.
- [19] I. S. Gradshteyn and I. M. Ryzhik, *Table of integrals, Series, and Products*, 7th ed. Academic Press, 2007.

- [20] A. M. Mathai, R. K. Saxena, and H. J. Haubold, *The H-function: Theory and Applications*. Springer Science & Business Media, 2009.
- [21] A. Papoulis and S. U. Pillai, *Probability, Random Variables, and Stochastic Processes*. McGraw-Hill Education, 2002.
- [22] M. C. Gursoy, D. Qiao, and S. Velipasalar, "Analysis of energy efficiency in fading channels under QoS constraints," *IEEE Trans. Wireless Commun.*, vol. 8, no. 8, pp. 4252–4263, Aug. 2009.
- [23] M.-S. Alouini and A. J. Goldsmith, "Capacity of Rayleigh fading channels under different adaptive transmission and diversity-combining techniques," *IEEE Trans. Veh. Technol.*, vol. 48, no. 4, pp. 1165–1181, Apr. 1999.
- [24] A. P. Prudnikov, J. A. Bryčkov, and O. I. Maričev, *Integrals and Series. Vol. 1, Elementary Function*, 1986.
- [25] A. A. Kilbas, *H-transforms: Theory and Applications*. CRC Press, 2004.
- [26] Wolfram, "The wolfram functions site," <http://functions.wolfram.com>.
- [27] A. J. Goldsmith and P. P. Varaiya, "Capacity of fading channels with channel side information," *IEEE Trans. Inf. Theory*, vol. 43, no. 6, pp. 1986–1992, Nov. 1997.
- [28] J. Cheng and T. Berger, "Capacity of a class of fading channels with channel state information (CSI) feedback," in *Proc. Allerton Conf. Commun. Control Comput.* Allerton Park, IL, Oct. 2001, pp. 1152–1160.
- [29] A. Goldsmith, *Wireless Communications*. Cambridge University Press, 2005.
- [30] M.-S. Alouini and A. J. Goldsmith, "Comparison of fading channel capacity under different CSI assumptions," in *Proc. IEEE Veh Technol. Conf.*, Sep. 2000, pp. 1844–1849.
- [31] A. P. Prudnikov, J. A. Bryčkov, and O. I. Maričev, *Integrals and Series. Vol. 3: More Special Functions*, 2003.
- [32] S. Al-Ahmadi and H. Yanikomeroglu, "On the approximation of the generalized- K distribution by a gamma distribution for modeling composite fading channels," *IEEE Trans. Wireless Commun.*, vol. 9, no. 2, pp. 706–713, Feb. 2010.